

Experimental Evaluation of Zp-Ofdm Scheme in Time Varying Underwater Multipath Channel

Rehan Khan, Qiao Gang and Asim Ismail

College of Underwater Acoustics Engineering, Harbin Engineering University, Harbin, P.R. China

Abstract: An experimental analysis to evaluate the practical suitability of the Underwater Acoustic (UWA) communication scheme is the major aim of this study. Oceanic channel imposes two major challenges (i.e., multipath propagation and Doppler effects) for underwater acoustic communication. Being fastest possible underwater information exchanger, OFDM is considered as the most viable option for mitigation of multipath. However, wideband nature of oceanic channel introduces severe Doppler shifts when dealing with OFDM subcarriers. Slight dynamics in a channel may cause overlapping of subcarriers such that entire signal can get completely distorted and sued as ICI (inter-carrier interference) induced transmission. In this study, we are presenting the algorithm to rectify the effects of Doppler shifts and to make OFDM technique more robust and more feasible for underwater environments. This study assures the performance of Zero-Padded Orthogonal Frequency Division Multiplexing (ZP-OFDM) based communication system in dynamic channel conditions. Data transmission using various packets structures are used to demonstrate the effectiveness of ZP-OFDM scheme. The narrow rectangular water tank of acoustic lab, Harbin Engineering University is utilized as a dynamic aquatic channel. The experimental results endorse the successful performance and suggest ZP-OFDM as a viable choice for high-rate communications over dynamic and high multipath oceanic channels.

Keywords: Doppler shift; multipath spread, Inter-Symbolic Interference (ISI), inter-carrier interference, Underwater Acoustic Communication (UWAC), Zero-Padded Orthogonal Frequency Division Multiplexing (ZP-OFDM)

INTRODUCTION

Transmitting underwater information with acoustic signals has been an interested research area for the experts, engineers and practitioners alike. Wireless acoustic communication can be used to gather data for various purposes like pollution control, climate monitoring, detection of objects on the ocean floor, transmission of images to distant sites on land, etc. Moreover; it is also useful for surveillance, remote sensing/ guidance and other military applications, as well as Autonomous Underwater Vehicles (AUVs) which could serve as mobile nodes in future Underwater Wireless Sensor Networks (UWSNs), Rehan *et al.* (2013b).

Oceanic channel is much more hostile as it has high absorption property thus, offers very limited bandwidth, unwanted multipaths from various boundaries and refraction of sound, dynamic responses for different temporal acoustic arrivals and slow speed of sound as compared to RF communication. These aspects make an underwater channel a very complex and high latent channel for acoustic communication, (Rehan *et al.*, 2011; Rehan and Qiao, 2013a).

Finding efficient techniques to communicate in such a channel has been an area of active research over the past several decades. Existing UWA communication relies on coherent single carrier modulation with decision feedback equalization to deal with the time-varying and highly dispersive UWA channels. Multipath propagation of an acoustic beam causes severe effects on communication and makes challenging for the appropriate design. The transmitted signal reflects many times from wavy sea surface, uneven bottom and other obstacles before reaching to the receiver. These delayed replicas cause destruction of the original signal in terms of Inter-Symbolic Interference (ISI). The chances of ISI are more dominant in long underwater channels having larger time delays as compared to RF channels. Since the frequency of the channel increases with the symbol rate, substantial rate improvement is impossible with single carrier modulation schemes. Multicarrier modulation schemes, on the other hand, convert a frequency selective channel into a set of flat fading channels, thus greatly simplifying the equalization process at the receiver. Therefore, to mitigate this effect, multicarrier modulation techniques have been implemented and successfully analyzed in oceanic

environments. Among multicarrier modulation schemes, OFDM is considered as the most viable solution for the UWAC (underwater acoustic communication). Cyclic Prefix (CP) and Zero Padded (ZP) based OFDM schemes have been used successfully in many researchers. In Taehyunk and Ronald (2008), Nejah *et al.* (2009) and Chitre *et al.* (2005), the authors have used CP concept to minimize the effect of ISI by converting linear convolution problem to the circular convolution problem. They found this approach very promising and effective i.e. can be handled through low complex equalization. Moreover, padding of zero bits instead of a cyclic prefix has been efficiently utilized in Li *et al.* (2008), Wang *et al.* (2010) and Parrish *et al.* (2008) to lessen the usage of unwanted power requirements.

Ocean dynamics is another major issue that causes mismatching between the local oscillators frequencies and therefore, adds non-uniform Doppler shifts in the original signal. These shifts further cause the temporal compression and expansion effects in the transmission waveforms. Although OFDM as a best suitable candidate to handle oceanic multipaths, these random dynamics destroy harshly the orthogonality among the subcarriers and introduce ICI (Inter-Carrier Interference). These distortions are non-uniform and extremely complex due to aquatic variations so, appropriate methods to overcome this sensitive problem are very essential. OFDM is considered very sensitive to Doppler spreading caused by surface wind or platform motion. To establish a ICI-free OFDM system against these variations, several schemes have been developed in recent times. Stojanovic (2006), for compensation of non-uniform Doppler shifts through pilot tone based phase tracking model, (Li *et al.*, 2008), for two-step approach and adaptive phase tracking model ink. Tu *et al.* (2009) are specifically considered.

In this study, we investigate the use of zero-padded OFDM for reliable design UWAC system in dynamic multipath environment. Zero-padding is used instead of a cyclic prefix to save the transmission power spent on the guard interval. For Doppler compensation, two-step approach is applied and tested successfully through underwater tank experiment. The main objective of this study is to evaluate and work out for the feasibility of ZP-OFDM scheme in the harsh and complex oceanic environments with dominant Doppler shifts. In this context, an experimental assessment of the aforementioned scheme has been carried out in the underwater tank of Acoustic laboratory of Harbin engineering university. The results show the convincing performance of the ZP-OFDM scheme with two step approach in the dynamic channel conditions.

MATHEMATICAL MODEL OF ZP-OFDM TRANSMISSION

Transmitter model: In OFDM modulation technique, available bandwidth is divided into several sub-carriers. The frequency spacing of the carriers is chosen in such a way that the modulated carriers are orthogonal and do not interfere with one another as shown in Fig. 1. The appropriate design of an OFDM with selection of a guard interval greater than the channel maximum delay may offer ISI-free communication. An OFDM based communication utilizes bandwidth efficiently and may increase the data rate significantly as compared to the conventional single carrier modulation based communication. The scheme is implemented by using simple fast Fourier transformation and successfully utilized for UWAC.

In the proposed OFDM based scheme; we consider T and T_g as the symbol time and guard interval

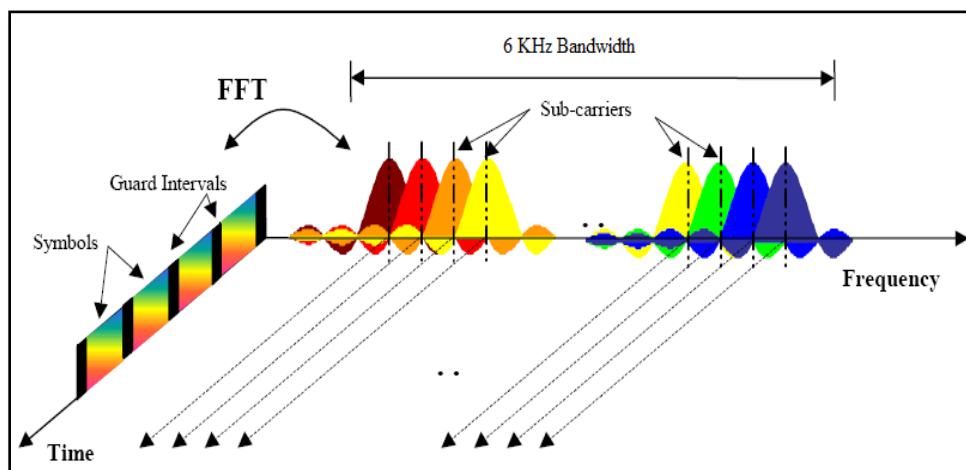


Fig. 1: OFDM modulation scheme

respectively. The total time OFDM block can be written as:

$$T_{total} = T + T_g$$

The frequency of each subcarrier is $\Delta f = \frac{1}{T}$ and the k^{th} subcarrier frequency is therefore be written as:

$$f_k = f_c + k\Delta f, k = -K/2, \dots, \dots, K/2 - 1 \quad (1)$$

where,

f_c = Carrier frequency
 K = The total number of subcarriers used in OFDM based communication. Bandwidth $B.W.$ is in relation with K as $B.W. = \frac{K}{T} = K\Delta f$, alternatively, from bandwidth we can derive, $\Delta f = \frac{B.W.}{K}$.

Total number of subcarriers are comprises of Pilot tones K_p and information bits K_s as:

$$K = K_s + K_p$$

The transmitting signal in pass-band can be written as:

$$s(t) = s_a(t) + s_g(t)$$

where, $s_a(t) = Re \left\{ \sum_k \left[d[k] e^{i2\pi k \frac{t}{T_{total}}} \right] e^{i2\pi f_c t} \right\}$, for $t \in \{0, T\}$ is the expression for OFDM symbol.

and, $s_g(t) = 0$ for $t \in \{T - T_g, T\}$, represents zero padding operation during guard interval time.

So, we can write complete expression for ZP-OFDM transmitting signal as:

$$s(t) = Re \left\{ \sum_k \left[d[k] e^{i2\pi k \frac{t}{T}} g(t) \right] e^{i2\pi f_c t} \right\} \quad (2)$$

where, $g(t) = 1$ for $t \in \{0, T\}$ & $g(t) = 0$ otherwise

We consider a dynamic multipath underwater channel in which each p^{th} path of total J Paths can be assumed to act like a low-pass filter. The expression for this channel impulse response can be written as:

$$h(\tau, t) = \sum_p A_p(t) \delta(\tau - \tau_p(t)) \quad (3)$$

where,

$A_p(t)$ = The path amplitude

$\tau_p(t)$ = The time varying path delay

The effects of oceanic dynamics/ platform motion in terms of Doppler shifting are modeled using Dopplerscale factor 'a' which scale time t to $t(1 + a)$. The time-varying path delay can be expressed in terms of Doppler factor as:

$$\tau_p(t) = \tau_p - a(t)t$$

To simplify our model and rectification of non-uniform wave motion, we assume all paths have same Doppler factor and path delays. τ_p , path gain A_p as well as Doppler factor a is constant over one symbol time as:

$$\tau_p(t) = \tau_p - at$$

Considering aforesaid assumptions, the overall impulse response will become:

$$h(\tau, t) = \sum_p A_p(t) \delta(\tau - \tau_p + at) \quad (3)$$

From the Doppler scale factor, each path is scaled in duration from T_{total} to $T_{total} / (1 + a)$, such that Doppler induced transmitted without multipath can be modeled as:

$$S_{Doppler}(t) = Re \left\{ \sum_{k \in K_A} \left[d[k] e^{i2\pi k \Delta f t (1+a)} \right] e^{i2\pi f_c t (1+a)} \right\};$$

for $t \in \{0, T\}$

With multipath channel, the Doppler induced receiving signal in baseband satisfies $\tilde{z}(t) = Re \{ z(t) e^{i2\pi f_c t} \}$ and can be written as:

$$z(t) = \sum_{k \in K_A} \left\{ \left[d[k] e^{i2\pi k \Delta f t} \times e^{i2\pi a f_c t} \right] \times \sum_{p=0}^{J-1} A_p e^{-i2\pi f_c \tau_p t + at - \tau_p + nt} \right\} \quad (4)$$

where, $\tilde{z}(t)$ = The passband version of receiving signal and $n(t)$ is the channel noise. In Fig. 2, block diagram of considered model of OFDM transmitter is shown.

Receiver model: In a receiver side, we first mitigate the effect of Doppler shifts and then drive the expression for the compensation of great multipath spread. In order to negate the frequency-dependent Doppler shifts, a two-step approach is adopted, which explained below as:

- First of all, resampling of the received pass-band signal is performed for the removal of Principal Doppler. Resampling with appropriate resampling factor rescales the waveforms and provides frequency-dependent Doppler compensation.

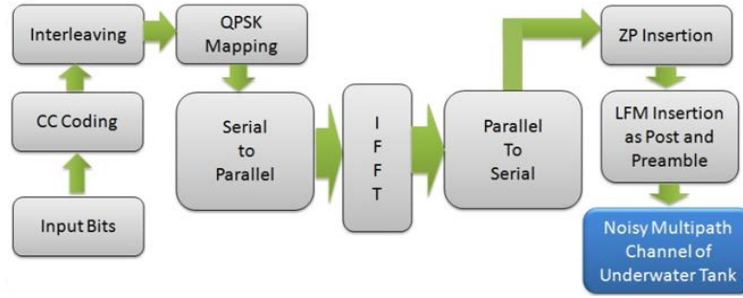


Fig. 2: Block diagram of implemented OFDM transmitter

- Resampling will transform ‘wideband’ problem into a ‘narrowband’ problem. The resampling parameter b should be selected such that:

$$\frac{1+a}{1+b} \approx 1$$

Resampling of pass-band signal $\tilde{z}(t)$ gives $\tilde{y}(t)$ as $\tilde{y}(t) = \tilde{z}\left(\frac{t}{1+b}\right)$, this corresponds and satisfies the resampled baseband signal $\tilde{y}(t) = \text{Re}\{y(t)e^{i2\pi f_c t}\}$ as:

$$y(t) = e^{i2\pi \frac{a}{1+b} f_c t} \sum_{k \in K_A} \left\{ d[k] e^{i2\pi k \Delta f \frac{1+a}{1+b} t} \times \right. \\ \left. p=0 \int A_p e^{-i2\pi f_k \tau_p} g(t - \tau_p + vt) \right\} \quad (5)$$

After resampling (5) becomes:

$$y(t) \approx e^{i2\pi \frac{a}{1+b} f_c t} \sum_{k \in K_A} \left\{ d[k] e^{i2\pi k \Delta f t} \times \right. \\ \left. p=0 \int A_p e^{-i2\pi f_k \tau_p} g(t - \tau_p + vt) \right\} \quad (6)$$

From (6), we can view the residual Doppler Effect is similar for all subcarriers. Hence, this narrowband expression only has frequency independent Doppler shifts.

- Subsequent to resampling step, high resolution uniform compensation on residual Doppler is carried out by modeling it as a CFO. This step corrects the residual Doppler shift finely to the ‘narrowband’ model and correspondingly used for best ICI reduction. Using a single CFO (ϵ) per OFDM symbol for Doppler compensation as:

$\epsilon = \frac{a}{1+b} f_c$ which further used for compensation of $y(t)$ as:

$$e^{-i2\pi \epsilon t} y(t) = \sum_{k \in K_A} \left\{ \left[\sum_{p=0}^J A_p e^{-i2\pi f_k \tau_p} g(t - \tau_p) \right] \right\} + \tilde{u}(t) \quad (7)$$

where $\tilde{u}(t) = e^{-i2\pi \epsilon t} v(t)$, the additive noise component and $t \in \{0, T\}$

For the removal of multipath effect, selection of an appropriate guard interval of duration T_g is used for the signal $y(t)$. The length of T_g be chosen such that it should be greater than the maximum delay of p^{th} path τ_{max} . The effects of various packet structures and respective length of zero padded guard intervals are analyzed in the next section. The compensated signal $\tilde{y}(t)$ is then in form of:

$$e^{-i2\pi \epsilon t} \tilde{y}(t) = \sum_{p=0}^J A_c \left\{ \sum_{k \in K_A} [d[k] e^{i2\pi k \Delta f t} g(t - \right. \\ \left. t_c \times e^{-i2\pi f_k t_c} + vt \right\} \quad (8)$$

where, $t_c = \tau_p + T_g$ is time such that, $y(t) = \tilde{y}(t)$ (i.e., compensated signal) for $T_g \geq \tau_p$, $A_c = A_p J - A_p N$ is an amplitude (N is number of compensated paths) and $v(t)$ is noise component after compensation of multipath spread respectively.

For the output of demodulator in the n^{th} subcarrier, the compensated signal can be written as:

$$y_n = \frac{1}{T} \int_0^T \tilde{y}(t) e^{-i2\pi(n\Delta f + \epsilon)t} dt \approx H(n)d[n] + u(n) \quad (9)$$

where, $H(n) = \sum_{p=0}^J h_p e^{-i2\pi f_k \tau_p}$ and $u(n)$ is the resultant noise.

Using energy of null subcarriers, CFO is eliminated out from y_n . After removal of ZP guard interval LS channel estimation is carried out in frequency domain. Moreover, proper equalization process, de-scaling and de-rotation of the received signal will restore the Orthogonality of the subcarriers used in ZP-OFDM. In Fig. 3, block diagram of implemented model of OFDM transmitter is shown.

PRACTICAL RECEIVER ALGORITHM

Figure 3 depicts the processing blocks of the proposed receiver. From the multipath and Doppler induced channel, received signals are directly

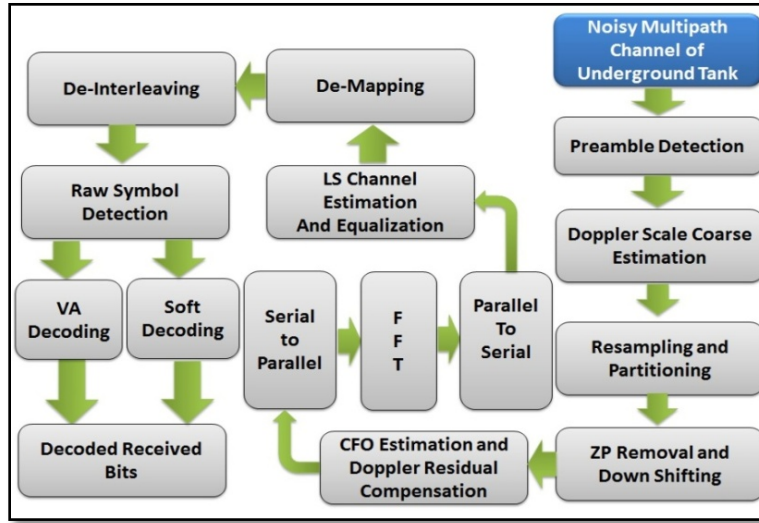


Fig. 3: Block diagram of implemented OFDM receiver

sampled for discrete-time entries post-processing procedures and uniform sampling time. Subsequently, the sampled signal is correlated with given preamble and post-amble to obtain Doppler scale coarse estimation. Resampling and portioning are carried out and principal Doppler free signal is achieved. Subsequent to cyclic prefix removal and downshifting, CFO estimation is carried out in a time domain for the removal of residual Doppler. VA (Viterbi Algorithm) decoding and soft (log-likelihood ratio -LLR) decoding schemes are used to analyze the decoded Bit Error Rates (BER).

Estimation of doppler scaling factor: Estimation of Doppler scaling factor a through resampling parameter b is carried out by cross correlating the received with known LFM sequences of Preamble and Post-amble. The resultant resampling parameter is obtained from the time duration of received signal T_{rx} and the known duration of transmitted signal T_{tx} . By comparing both time durations, the receiver reveals a guess of expansion or compression that the data packet has undergone. This information can be used to get an estimate of the relative Doppler shift and thus receiver resamples the signal as:

$$b \approx \tilde{a} = 1 - \frac{T_{tx}}{T_{rx}} \quad (10)$$

Estimation of Carrier Frequency Offset (CFO): The null carriers are used to estimate residual CFO for each OFDM symbol within a block. From (6), the expression for received signal after resampling, we collect $K + L$ samples as $\mathbf{y}(\mathbf{k}) = [\mathbf{y}(0), \dots, \dots, \mathbf{y}(K + L - 1)]^T$, where, $L + 1$ is assumed channels taps in discrete time. As assumed before, the OFDM symbol consists of K_A

active carriers and K_N null subcarriers out of a total of K subcarriers. Let us define null subcarrier's vector \mathbf{w}_n of size $(K + L) \times 1$ as $\mathbf{w}_n = \begin{bmatrix} 1, e^{i2\pi n/K}, \dots, \dots, e^{i2\pi n(K+L-1)/K} \end{bmatrix}^T$ and $(K + L) \times (K + L)$ diagonal matrix $\mathbf{E}(\varepsilon) = \text{diag} \left(1, e^{i2\pi \varepsilon T / K}, \dots, \dots, e^{i2\pi (K+L-1)\varepsilon T / K} \right)$. Matrix $\mathbf{E}(\varepsilon)$ represents CFO component which destroys the orthogonality of subcarriers. To hold the condition of orthogonality we can nullify CFO hypothetically as:

$$\mathbf{w}_n^H \mathbf{E}^H(\varepsilon) \mathbf{y}(k) = 0$$

This fact allows us to define cost function as:

$$Q(\varepsilon) = \sum_{n \in K_N} \sum_{k \in K} \|\mathbf{w}_n^H \mathbf{E}^H(\varepsilon) \mathbf{y}(k)\|^2 \quad (12)$$

The correct compensation of CFO will provide ICI free subcarriers hence, residual Doppler can be excreted in this manner from OFDM based UWAC. In order to find estimated CFO($\hat{\varepsilon}$), two dimensional search of the below expression has been made:

$$\hat{\varepsilon} = \text{abs}[\min_{\varepsilon} Q(\varepsilon)] \quad (13)$$

Pilot tone based channel estimation with relevant mathematical expression: Considering the assumption that Doppler scale factor is constant over one symbol time, ICI will be greatly reduced through resampling and CFO compensation. Pilot tone based Least Square (LS) method is used here to estimate the channel impulse response. From (9) we can relate the compensated signal at n^{th} subchannel as:

$$y_n = \text{fft}[y(k)] \mathbf{E}^H(-\hat{\varepsilon}) = H(n)d[n] + u(n) \quad (14)$$

where, $H(n)$ = The channel frequency response $u(n)$ = AWGN.

The coefficient of $H(n)$ can be related to the equivalent discrete-time baseband channel parameterized by $L + 1$ complex-valued coefficients as:

$$H(n) = \sum_{l=0}^L h_l e^{i2\pi ln/K} \quad (15)$$

We use K_p pilot symbols as the phase shift key (PSK) signals having equal spacing within K subcarriers. Ignoring noise component, the frequency-domain channel estimation is carried out by LS method on pilot symbols as:

$$H(p) = \frac{Y_p}{D_p} \quad (16)$$

where, $Y_p = y_n(p)$

$p \in K_p$ and D_p = The known pilot symbols

Using linear or any suitable method of interpolation $H(n)$ can be found for all information subcarriers K_s per symbol. Accordingly, data bits for n^{th} subchannel are obtained as:

$$D(n) = \frac{y_n(n)}{H(n)}, n \in K_s \quad (17)$$

PERFORMANCE RESULTS FOR THE EXPERIMENT IN WATER POOL

The configuration of water pool experimental present in Harbin Engineering University is shown in Fig. 4.

For the water pool experiment, the selected bandwidth of OFDM scheme is B. W. = 6K Hz and the

carrier frequency is $f_c = 48\text{KHz}$. ZP (zero-padded) OFDM of 256, 512 and 1024 subcarriers with the guard interval of $T_g = 1.354 \text{ ms}$, $T_g = 2.708 \text{ ms}$ and $T_g = 5.147 \text{ ms}$, respectively per OFDM symbols are chosen. The subcarriers spacing and OFDM blocks duration $\Delta f = 23.44\text{Hz}$, 11.72Hz , 5.86Hz and $T = 42.7 \text{ ms}$, 85.3 ms , 170.6 ms are considered for respective packet structures. Convolution coding of rate $\frac{1}{2}$ with constraint length of 14 and generator polynomial of (21675,27123) is applied within the data stream for all OFDM blocks. The 10 m channel range is selected with the depths of both transmitter and receivers are 1meter. Underwater transducer is moving using a pulley with an approximate speed of two Knots. Number of equally spaced Pilot and start-end positioned null bits (for compensation of channel dynamics, i.e., Doppler Effect) are selected using:

$$K_p = K/4 = 64 \text{ bits/symbol}$$

$$\text{And, } K_N = K/18 \approx 14 \frac{\text{bits}}{\text{symbol}} \text{ (null subcarriers is utilized for CFO estimation)}$$

The total numbers of information (input) bits to be transmitted in an OFDM packet are 1024, 2048 and 4096, respectively for 256 bits to 1024 frame structures.

Moreover, two compressed image files are transmitted underwater to see the visual effect. Thus, various configurations of ZP OFDM with respect to the frames and symbols sizes are considered in our study.

QPSK mapping using MATLAB built-in command and modem. pskdemod modem.pskdemod is implemented with the aim to obtain the appropriate results. Table 1 shows the similar theoretical data rates

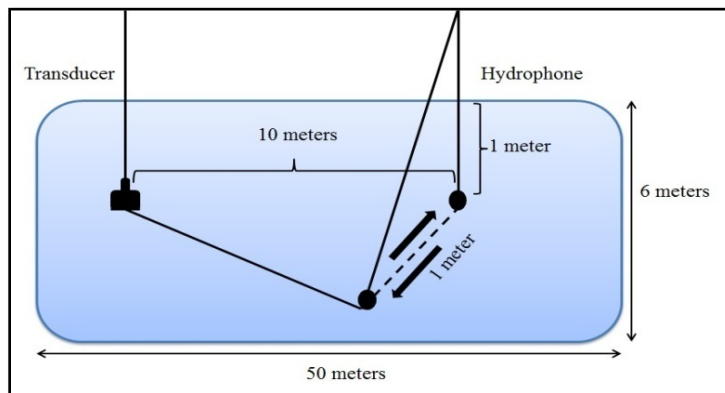


Fig. 4: Experimental setup

Table 1: Parameters and respective data rates

No. of Active Subcarriers K_A	Data Bits rates without coding $\frac{2(K_A - K/4)}{T_{total}}$	With $\frac{1}{2}$ rate CC coding	Remarks ($T_g = T_{total} / 4$)
256	8.73 Kbps	4.36 Kbps	$T_g = 1.354 \text{ ms}$
512	8.73 Kbps	4.36 Kbps	$T_g = 2.708 \text{ ms}$
1024	8.73 Kbps	4.36 Kbps	$T_g = 5.147 \text{ ms}$

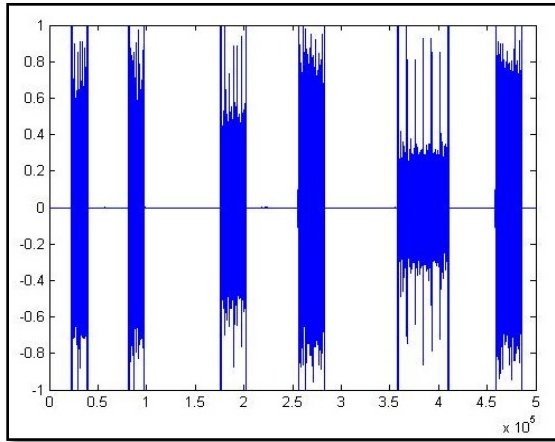


Fig. 5: Transmitted burst structure

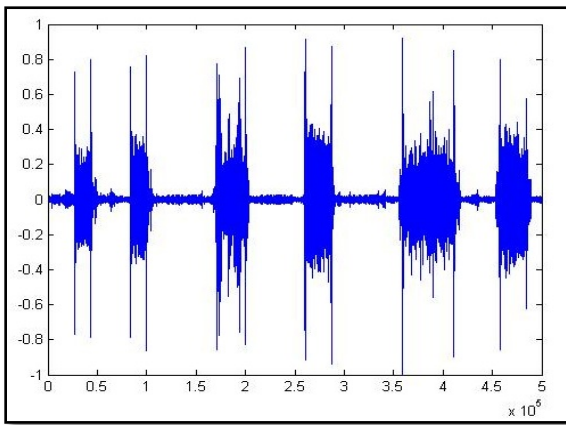


Fig. 6: Receiving burst (256 bits packet to 1024 bits packet)

obtained from various frame structures (i.e., fixed length of a guard interval $\approx \frac{1}{4^{\text{th}}}$ of T_{total} is considered.)

Transmitted signal burst structure is shown in Fig. 5, where various packets are transmitted in the sequential way and similarly processed in the receiver side.

Receiving burst is shown in the Fig. 6, where pairs of 256 bits (first two), 512 bits (middle two) and 1024 bits (last two) packets are received in the same manner. Two compressed images are also sent to check the effect of multipath on these three configurations.

LFM correlation results for Preamble and Postamble detection and synchronization of packets in all three configurations are shown in Fig. 7a to c.

Doppler scaling factor estimation and CFO Tracking: Using preamble and post-amble detection Doppler scale factor is estimated and the receiving signal is processed for deletion of Principal Doppler. From equation 13, CFO is calculated to mitigate the effect of residual Doppler. Assuming, $V_{\text{sound}} = 15000\text{m/s}$, the velocity of transmitted signal V_{wave} can be calculated as:

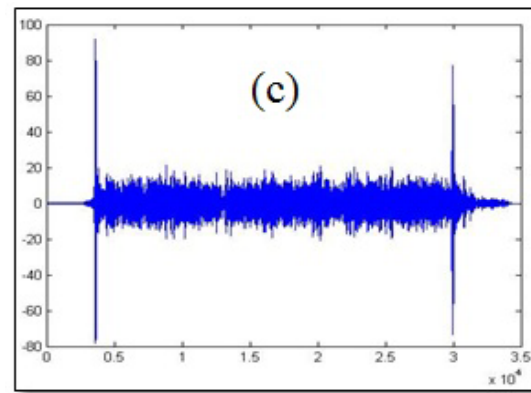
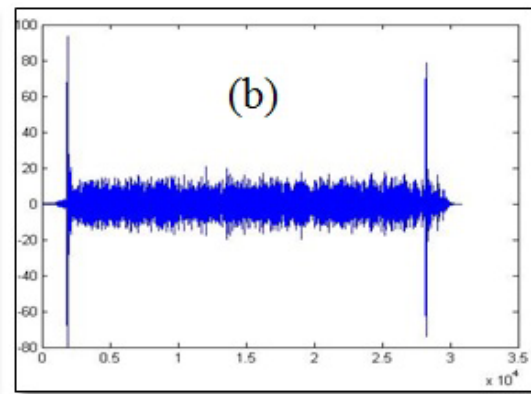
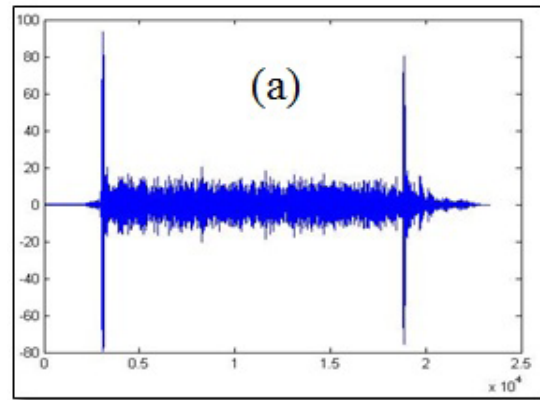


Fig. 7: LFM correlation (a. 256 bits, b. 512 bits and c. 1024 bits)

$$V_{\text{wave}} = \{CFO / (CFO + f_c)\} V_{\text{sound}} \times 1.943 \text{ (knots)}$$

CFO tracking is properly done and the same is endorsed in Fig. 8a to c i.e., tracked CFO with respect to the relative velocity between the transmitter and receiver. Relative velocity V_{wave} estimated from tracked CFO is almost same as the actual speed of moving hydrophone.

LS channel estimation and symbol detection: Channel estimated impulse responses on first (blue) and

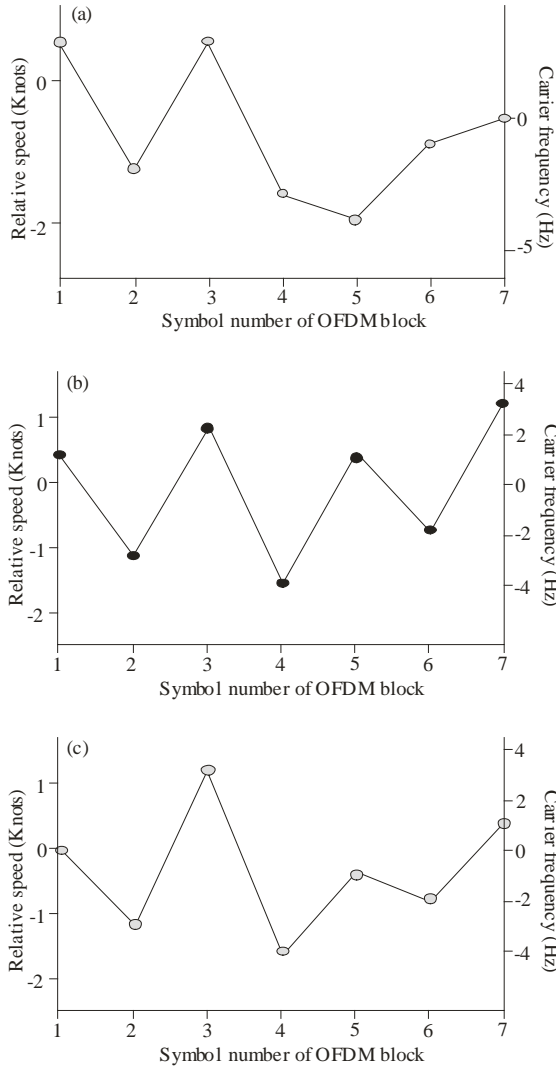


Fig. 8: CFO Tracking w.r.t. relative velocities (a. 256 bits, b. 512 bits and c. 1024 bits)

last (green) symbols obtained from the least square method for all three configurations are shown in Fig. 9a to c. The plots explained almost similar channel responses estimated on first and the last symbols in all packet's structures that further endorsed the robustness of an OFDM scheme with LS- estimation.

Scatter plots of demodulated (QPSK) receiving bits are shown in Fig. 10a to c respectively for the 256 bits, 512 bits and 1024 bits packet structures. Response from scattered plots explains that the decision points are more prominent in second and third cases however, for first, case decision points are not cleared. These plots explained the selection of guard interval length as for 256 bits packet, the length of a guard interval is only $T_g = 1.354 \text{ ms}$ (i.e., more chances of $T_g < \tau_{max}$).

Better results are depended upon the selection of guard interval length and Doppler mitigation technique. From the scatter plots and the experiment setup, we can

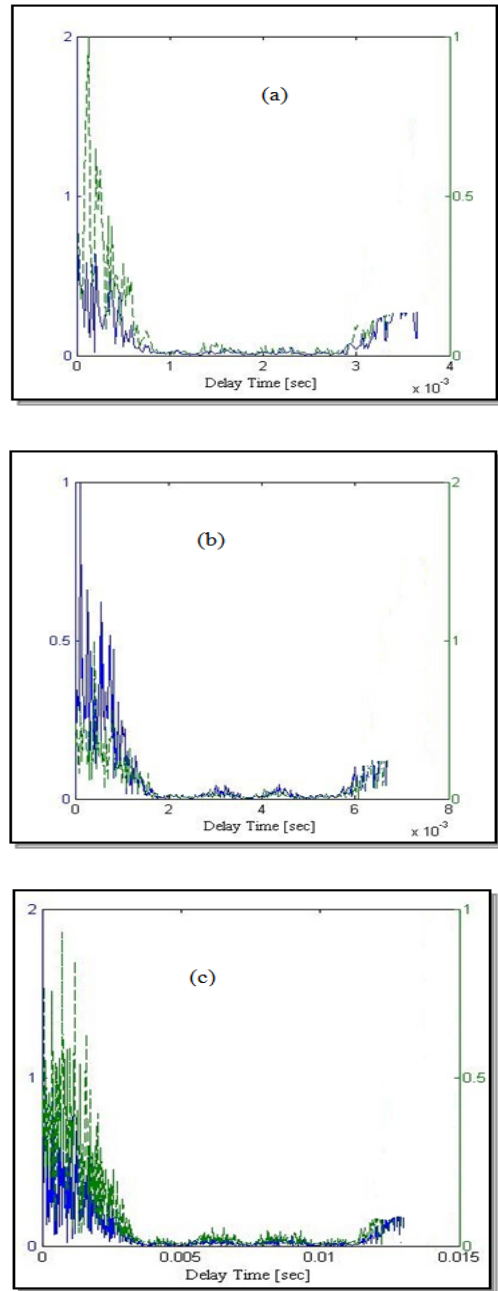


Fig. 9: Estimated channel (a. 256, b. 512 and c. 1024 bits)

say that perfect mitigation of multipath effect will be achieved when CFO is able to track the variations and endorsed the effects of actual speed of relative motion, moreover, the proper selection of guard interval i.e. T_g (approx) $\geq 15 \text{ ms}$ for this underwater channel. However, tradeoff has to be considered between the bit data rate and the level of compensation of multipath. For instance if we consider $T_g \approx 15 \text{ ms}$, raw data rate will be dropped i.e. It will become 6.6, 7.6 and 8.2 Kbps, respectively for 256, 512 and 1024 bits, respectively frame structures. The degradation

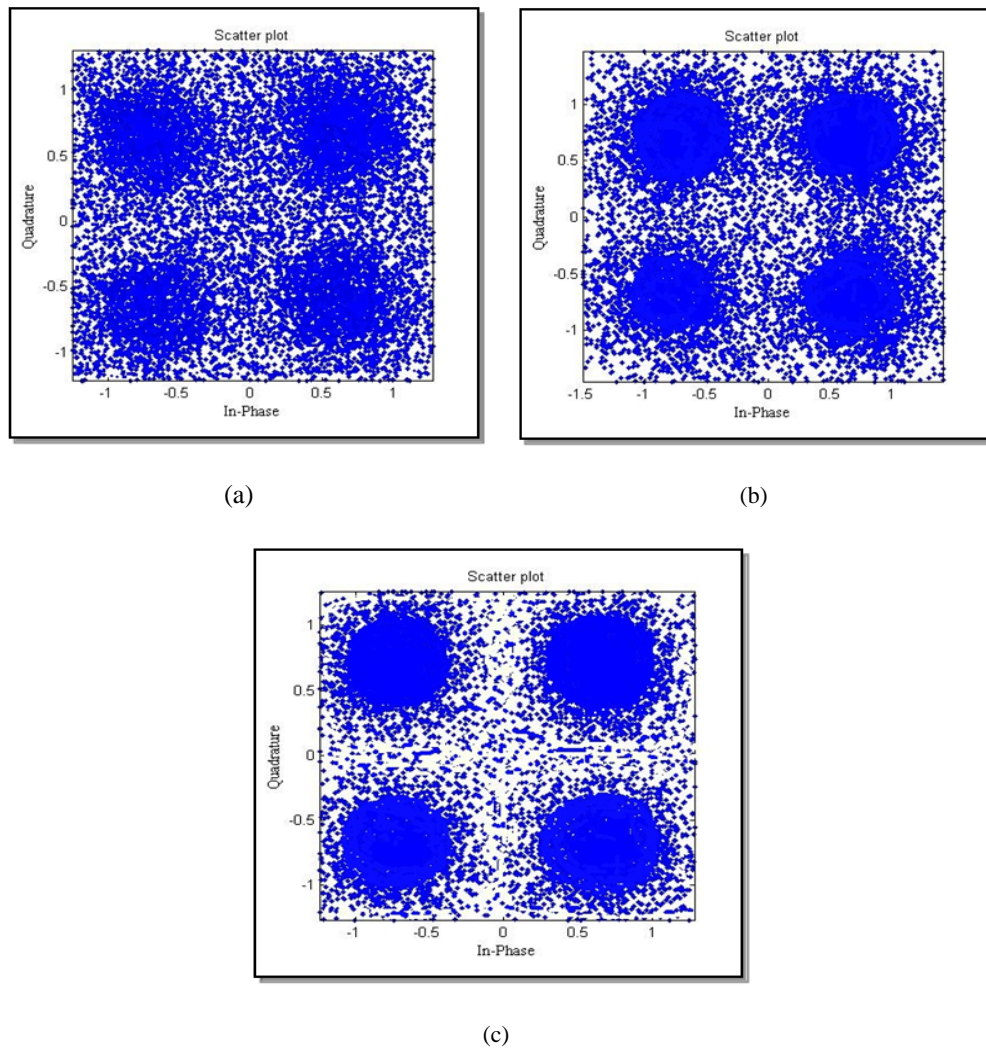


Fig. 10: Scatter plot (a. 256, b. 512 and c. 1024 bits)

Table 2: BER for the image transmissions

ZP-OFDM Transmission	256 Bits/ symbol frame		512 Bits/ symbol frame		1024Bits/ symbol frame	
	Raw	Dec	Raw	Dec	Raw	Dec
Image 1Transmission	~0.122	~0.180	~0.073	~0.009	~0.017	0
Image 2Transmission	~0.142	~0.187	~0.081	~0.014	~0.019	0

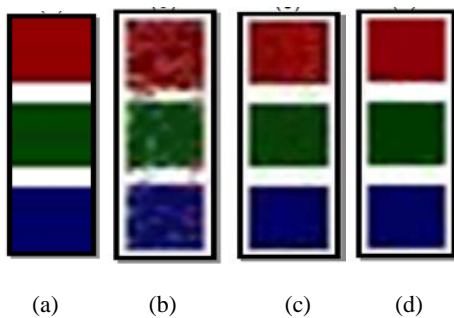


Fig. 11: Transmitted image 1 (Left to right: Original, 256, b. 512 and c. 1024 bits)

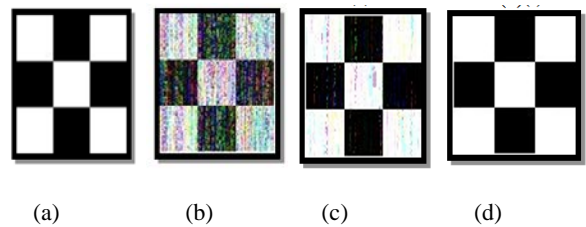


Fig. 12: Transmitted image 2 (Left to right: Original, 256, b. 512 and c. 1024 bits)

effects induced by channel and their compensation are further elaborated in the Fig. 11 and 12:

It is cleared from the image transmission that the degradation effects are very much dominant in 256 bits frame having very small guard interval length. Details of raw and decoded bit error rates are illustrated below in the Table 2.

CONCLUSION

In this study, we have presented the performance evaluation of ZP-OFDM based scheme for the two major problems incurred in an oceanic channel. Two-step approach is adopted here to mitigate the effect of Doppler shifts and ICI-free communication is effectively tested on the dynamic multipath channel of the water tank of Harbin engineering University. From the experimental results, it is revealed that implemented scheme has a capability to track the CFO occurred due to the relative motion and with proper selection of a guard interval it may provide error-free communication. Out of three frame structures, 1024 bits/ symbol frame is considered suitable for the given channel as it provides higher data rate (i.e. 8.72 Kbps raw and 4.36 Kbps coded) i.e. with zero decoded BER. Proper tradeoff between data rate and the BER is an essential parameter to be measured while developing OFDM based communication system.

This technique will be examined in the lake/ sea experiments for further improvements and as a part of future research work.

ACKNOWLEDGMENT

The author is very thankful to faculty of Underwater Acoustic lab, Harbin Engineering University for the allowing an experimental setup, Prof. Qiao Gang for his valuable supervision and his colleagues for their precious guidelines for this study.

REFERENCES

Chitre, M., S.H. Ong and J. Potter, 2005. Performance of coded OFDM in very shallow water channels and snapping shrimp noise. *Proceeding of MTS/IEEE OCEANS*. Washington, DC, 2: 996-1001.

Li, B., S. Zhou, M. Stojanovic, L. Freitag and P. Willett, 2008. Multicarrier communication over underwater acoustic channel with nonuniform doppler shifts. *IEEE J. Ocean Eng.*, 33(2): 198-209.

Nejah, N., A. Laurent, K. Abdennaceur and S. Mounir, 2009. Behavioral modeling and simulation of underwater channel. *J. WSEAS Trans. Commun.*, 8(2): 259-268.

Parrish, N., S. Roy and P. Arabshahi, 2008. Poster abstract: OFDM in underwater channel. *Proceeding of the 3rd ACM Workshop on Underwater Networks (Mobicom)*. San Francisco, CA.

Rehan, K., G. Qiao and W. Wang, 2011. A review of underwater acoustic communication techniques. *Proceeding of 3rd International Conference on Mechanical and Electrical Technology (ICMET)*. China, pp: 151-158.

Rehan, K. and G. Qiao, 2013a. A survey of underwater acoustic communication and networking techniques. *Res. J. Appl. Sci. Eng. Technol.*, 5(3): 778-789.

Rehan, K., G. Qiao, I. Asim and M. Khurram, 2013b. Investigation of channel modeling and simulation of OFDM based communication near Northern Regions of Arabian Sea. *Res. J. Appl. Sci. Eng. Technol.*, 5(4): 1169-1182.

Stojanovic, M., 2006. Low complexity OFDM detector for underwater acoustic channels. *Proceeding of IEEE OCEANS Conference*, pp: 1-6.

Taehyunk, K. and A.L. Ronald, 2008. Matching pursuits channel estimation for an underwater acoustic OFDM modem. *Proceeding of IEEE International Conference on Acoustics, Speech and Signal Processing (ICASSP)*, pp: 5296-5299.

Tu, K., D. Fertoni, T.M. Duman and P. Hursky, 2009. Mitigation of intercarrier interference in OFDM systems over underwater acoustic channels. *Proceeding of Conference on OCEANS*, Department of Electr. Eng. Arizona State University, Tempe, AZ, USA, pp: 1-6.

Wang, Z., S. Zhou, G.B. Giannakis, C.R. Berger and J. Huang, 2010. Frequency-domain oversampling for zero-padded OFDM in underwater acoustic communication. *Proceeding of IEEE Global Telecommunications Conference (GLOBECOM 2010)*, pp: 1-5.